

# An Integrated Approach to Produce Robust Models with High Efficiency

Zhijian Li, Bao Wang, and Jack Xin

**Abstract**—Deep Neural Networks (DNNs) needs to be both efficient and robust for practical uses. Quantization and structure simplification are promising ways to adapt DNNs to mobile devices, and adversarial training is the most popular method to make DNNs robust. In this work, we try to obtain both features by applying a convergent relaxation quantization algorithm, Binary-Relax (BR), to a robust adversarial-trained model, ResNets Ensemble via Feynman-Kac Formalism (EnResNet). We also discover that high precision, such as ternary (tnn) and 4-bit, quantization will produce sparse DNNs. However, this sparsity is unstructured under adversarial training. To solve the problems that adversarial training jeopardizes DNNs' accuracy on clean images and the structure of sparsity, we design a trade-off loss function that helps DNNs preserve their natural accuracy and improve the channel sparsity. With our trade-off loss function, we achieve both goals with no reduction of resistance under weak attacks and very minor reduction of resistance under strong attacks. Together with quantized EnResNet with trade-off loss function, we provide robust models that have high efficiency.

## I. INTRODUCTION

### A. Background

Deep Neural Networks (DNNs) has achieved significant success in computer vision. Especially, the residual network (ResNet)[9] has state-of-the-art performance on image classification and has become one of the most important Neural Network architecture in current literature. Despite the large success of CNN, researchers still try to strength two properties of DNNs, robustness and efficiency. Robustness keeps the model accurate under small perturbation of input images, and efficiency can fit DNNs into embedded system, such as smartphone. Many defensive methods [17], [8], [13], [28] have been invented to increase the robustness of Neural Network. Among them, Projected Gradient Decent (PGD) [17] training is one of the most effective and powerful method. Meanwhile, several attack methods [7], [3], [1], [2] are proposed to examine the robustness of models. Fast Gradient Sign Method (FGSM) and iterative FGSM [7] are amongst widely used to test the robustness of models by researchers. On the other hand, quantization [5], [19], producing models with low-precision weights, and structured simplification, such as channel pruning [10], [29], are promising ways to make models efficient. Both methods above can significantly accelerate DNNs and reduce the memory sources required

### B. Our Contributions

Based on related works, we study the robustness of binary models under PGD training. We try to find the possibility to

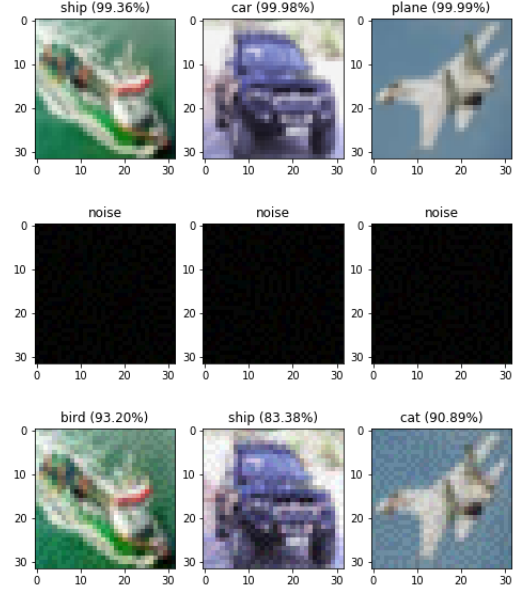


**Fig. 1:** First row: the original image labeled with the classification of a ResNet56 and its confidence level. Second row: the perturbation (noise) generated by FGSM labeled with the classification of the model and its confidence level

meet both robustness and efficiency, as well as the balance of natural accuracy and robust accuracy. Our work involves in both experimental investigation and theoretical analysis.

- Experimentally, we find that EnResNet is able to maintain high robustness with binary weights. We also show that the model trained by Binary-Relax [27] algorithm has better natural accuracy and robust accuracy than that trained by traditional Binary-Connect (BC) [5] algorithm.
- We make an improvement on the trade-off loss function initially proposed by [28], which increases both natural accuracy and robust accuracy. We also provide theory that can potentially explain why the improved trade-off loss function performs better.
- We discover that high precision quantization produces sparse DNNs. We also investigate the structure of the sparsity and provide a method to produce quantized robust models with structured sparsity that can be further simplified by channel pruning.

## II. RELATED WORK

### A. Binary Quantization

Based on BC, [27] proposed a improvement of BC called Binary-Relax, which makes the weights converge to binary

from float gradually. Theoretically, [27] provided the convergence analysis of BC, and [14] presented an ergodic error bound of BC. The space of  $m$ -bit quantized weights  $\mathcal{Q} \subset \mathbb{R}^n$  is a union of disjoint one-dimensional subspace of  $\mathbb{R}^n$ .

$$\mathcal{Q} = \mathbb{R}_+ \times \{\pm q_1, \dots, \pm q_m\}^n = \bigcup_{l=1}^p \mathcal{A}_l$$

We minimize our object function in the subspace  $\mathcal{Q}$ . Hence, the problem of binarizing weights can be formulated in two equivalent forms:

$$\operatorname{argmin}_{u \in \mathcal{Q}} \mathcal{L}(u)$$

$$\operatorname{argmin}_{u \in \mathbb{R}^n} \mathcal{L}(u) + \chi_{\mathcal{Q}}(u) \quad \text{where} \quad \chi_{\mathcal{Q}}(u) = \begin{cases} 0 & u \in \mathcal{Q} \\ \infty & \text{else} \end{cases} \quad (1)$$

Based on the alternative form, [27] relaxed the optimization problem to:

$$\operatorname{argmin}_{u \in \mathbb{R}^n} \mathcal{L}(u) + \frac{\lambda}{2} \operatorname{dist}(u, \mathcal{Q})^2 \quad (2)$$

Observing (2) converges to (1) pointwise as  $\lambda \rightarrow \infty$ , [27] proposed a relaxation of BC:

$$\begin{cases} w_{k+1} = w_k - \gamma \nabla \mathcal{L}(u_k) \\ u_{k+1} = \operatorname{argmin}_{u \in \mathbb{R}^n} \frac{1}{2} \|w_{k+1} - u\|^2 + \frac{\lambda}{2} \operatorname{dist}(u, \mathcal{Q})^2 \end{cases}$$

where the second step is solved in closed form:

$$\begin{aligned} u_{k+1} &= \operatorname{argmin}_{u \in \mathbb{R}^n} \frac{1}{2} \|w_{k+1} - u\|^2 + \frac{\lambda}{2} \operatorname{dist}(u, \mathcal{Q})^2 \\ &= \frac{\lambda \operatorname{proj}_{\mathcal{Q}}(w_{k+1}) + w_{k+1}}{\lambda + 1} \end{aligned}$$

---

#### Algorithm 1 Binary-Relax quantization algorithm

---

- 1: **Input:** mini-batches  $\{(\mathbf{x}_1, \mathbf{y}_1), \dots, (\mathbf{x}_m, \mathbf{y}_m)\}$ ,  $\lambda_0 = 1$ , growth rate  $\rho > 1$ , learning rate  $\gamma$ , initial float weight  $w_0$ , initial binary weight  $u_0 = w_0$ , cut-off epoch  $M$
  - 2: **Output:** a sequence of binary weights  $\{u_t\}$
  - 3: **for**  $t = 1, \dots, N$  **do**  $\triangleright N$  is the number of epochs
  - 4:   **if**  $t < M$  **then**
  - 5:     **for**  $k = 1, \dots, m$  **do**
  - 6:        $w_t = w_{t-1} - \gamma_t \nabla \mathcal{L}(u_{t-1})$
  - 7:        $u_t = \frac{\lambda_t \cdot \operatorname{Proj}_{\mathcal{Q}}(w_t) + w_t}{\lambda_t + 1}$
  - 8:        $\lambda_{t+1} = \rho \cdot \lambda_t$
  - 9:   **else**
  - 10:     **for**  $k = 1, \dots, m$  **do**
  - 11:        $w_t = w_{t-1} - \gamma_t \nabla \mathcal{L}(u_{t-1})$
  - 12:        $u_t = \operatorname{Proj}_{\mathcal{Q}}(w_t)$   $\triangleright$  This is precisely Binary-Connect
  - 13: **return** quantized weights  $u_N$
- 

#### B. Adversarial Attacks

As [21] discovered the limited continuity of DNNs' input-output mapping, the outputs of DNNs can be changed by adding fairly small perturbations to input data. The methods that generate perturbed data are adversarial attacks, and the generated perturbed data are called adversarial examples. Here we introduce three adversarial attacks:

##### 1) Fast Gradient Sign Method (FGSM):

Given a specific magnitude of perturbation  $\epsilon$ , FGSM searches adversarial examples by perturb the input data towards gradient of loss function.

$$x' = x + \epsilon \cdot \nabla_w \mathcal{L}(f(w, x), y)$$

##### 2) Iterative FGSM (IFGSM)

Given a iteration number  $n$ , step size  $\alpha$ , and a magnitude  $\epsilon$ , IFGSM generates adversarial examples by perturb the data towards the gradient of loss function iteratively and threshold the perturbation.

$$x^{(n)} = x^{n-1} + \alpha \nabla_w \mathcal{L}(f(w, x^{(n-1)}), y)$$

for  $n = 1, \dots, n$ , and  $x^{(0)} = x$ . Then,

$$x' = x + \operatorname{Clip}_{\epsilon}(x^{(n)})$$

##### 3) Carlini and Wagner method (C&W):

C&W method provides adversarial examples by solving the problem

$$\min_{\delta} \|\delta\| \quad \text{s.t.} \quad f(w, x + \delta) = t$$

for a target label  $t$ . While Carlini and Wagner originally proposed the metric  $\|\cdot\|$  to be  $l_2$ , most researchers use  $l_{\infty}$  instead. In our study, we also use  $l_{\infty}$  for C&W attack.

Among these 3 adversarial attacks, IFGSM is the strongest attack. IFGSM can make a ResNet56 with natural training predict all test data of Cifar10 wrong with confidence level at least 99.3% over all test images. C&W can reduce the test accuracy of ResNet56 on Cifar10 from 92% to 5.12%, and FGSM reduces the accuracy to 17.26%. While there are many more adversarial attack methods [12], [15], methods above are computationally efficient and are the most popular methods used to examine the robustness of models.

#### C. Adversarial Training

Adversarial training [1], [17] generates perturbed input data and train the model to stay stable under adversarial examples. It has object function:

$$\min_w \mathcal{L}(w) = \frac{1}{N} \sum_{n=1}^N \max_{\tilde{x}_n \in D_n} l(f(w, \tilde{x}_n), y_n) \quad (3)$$

where  $D_n = \{x \mid \|x - x_n\|_{\infty} < \delta\}$ .  $l$  and  $f$  are the loss function and the DNN respectively. A widely used method to practically find  $\tilde{x}_n$  is PGD [17]. [28] shows that adversarial training with PGD is, in general, more powerful than other methods such as gradient mask and gradient regularization [13]. [20] investigated the properties of the object function of adversarial training, and [25] provided convergence analysis of adversarial training based on the previous.

**Feynman-Kac formalism principled Robust DNNs:** Neural ordinary differential equations (ODEs) [4] are a class of DNNs that use an ODE to describe the data flow of each input data. Instead of focusing on modeling the data flow of each individual input data, [24], [23], [16] use a transport equation (TE) to model the flow for the whole input distribution. In particular, from the TE viewpoint, [24] modeled training ResNet [9] as finding the optimal control of the following TE

$$\begin{cases} \frac{\partial u}{\partial t}(\mathbf{x}, t) + G(\mathbf{x}, \mathbf{w}(t)) \cdot \nabla u(\mathbf{x}, t) = 0, & \mathbf{x} \in \mathbb{R}^d, \\ u(\mathbf{x}, 1) = g(\mathbf{x}), & \mathbf{x} \in \mathbb{R}^d, \\ u(\mathbf{x}_i, 0) = y_i, & \mathbf{x}_i \in T, \end{cases}$$

with  $T$  being the training set.

where  $G(\mathbf{x}, \mathbf{w}(t))$  encodes the architecture and weights of the underlying ResNet,  $u(\mathbf{x}, 0)$  serves as the classifier,  $g(\mathbf{x})$  is the output activation of ResNet, and  $y_i$  is the label of  $\mathbf{x}_i$ .

[24] interpreted adversarial vulnerability of ResNet as arising from the irregularity of  $u(\mathbf{x}, 0)$  of the above TE. To enhance  $u(\mathbf{x}, 0)$ 's regularity, they added a diffusion term,  $\frac{1}{2}\sigma^2\Delta u(\mathbf{x}, t)$ , to the governing equation of (4) which resulting in the convection-diffusion equation (CDE). By the Feynman-Kac formula,  $u(\mathbf{x}, 0)$  of the CDE can be approximated by the following two steps:

- Modify ResNet by injecting Gaussian noise to each residual mapping.
- Average the output of  $n$  jointly trained modified ResNets, and denote it as  $\text{En}_n\text{ResNet}$ .

[24] have noticed that  $\text{EnResNet}$  can improve both natural and robust accuracies of the AT DNNs. In this work, we leverage the sparsity advantage of  $\text{EnResNet}$  to push the sparsity limit of the AT DNNs.

### III. QUANTIZATION OF ENRESNET

We know that the accuracy of a quantized model will be lower than its float equivalent because of loss of precision. However, we want to know that whether a quantized model is more vulnerable than its float equivalent under adversarial attacks? In this section, we study this question by comparing the accuracy drops of the natural accuracy and robust accuracy from float weights to binary weights. Meanwhile, we also investigate the performances between two quantization methods BC and BR.

#### A. Experimental Setup

**Dataset.** We use one of the most popular dataset CIFAR-10 [11] to evaluate the quantized models, as it would be convenient to compare it with the float models in [24], [28].

**Baseline.** For model, our baseline model is the regular ResNet. Since, as the best of our knowledge, there are no suitable work done before that investigated the robustness of models with quantized weights. We mainly look at that how close our quantized models can be to the float models [24], [28].

**Evaluation.** We evaluate both natural and robust accuracies for quantized adversarial trained models. We examine the robustness of models by three attack methods, FGSM ( $A_1$ ), iterative FGSM ( $A_2$ ), and C&W ( $A_3$ ). In our recording,  $N$  denotes the natural accuracy (accuracy on clean images) of

models. For algorithm, we set Binary-connect as our baseline, we want see that the advantage of the relaxed algorithm 1 in [27] is preserved under adversarial training. We use the wildly used binarizing projection proposed by [19], namely:

$$\text{Proj}_{\mathcal{Q}}(w) = \mathbb{E}[|w|] \cdot \text{sign}(w) = \frac{\|w\|_1}{n} \cdot \text{sign}(w)$$

where  $\text{sign}(\cdot)$  is the component-wise sign function and  $n$  is the dimension of weights.

#### (4) B. Result

First, we see that the quantized models can maintain decent robustness under the attacks. The drops of the robust accuracies are roughly in the same amount as the natural accuracy (Table I), which indicates that quantization does not make the model more vulnerable.

Second, we investigate the performances of Binary-Connect method (BC) and Binary-Relax method (BR). We verify that BR outperforms BC (Table I). A quantized model trained via BR provides higher natural accuracy and robust accuracy. As a consequence, we use this relaxed method to quantize DNNs in all subsequent experiments in this paper.

Finally, We verify that the  $\text{EnResNet}$  is more robust com-

net	quant	$N$	$A_1$	$A_2$	$A_3$
En <sub>1</sub> ResNet20	float	78.31%	56.64%	49.00%	66.84%
	BC	68.84%	46.31%	42.45%	58.52%
	BR	69.60%	47.17%	43.89%	58.79%
En <sub>2</sub> ResNet20	float	80.10%	57.48%	49.55%	66.73%
	BC	71.48%	47.83%	43.03%	59.09%
	BR	72.58%	49.29%	44.72%	60.36%
En <sub>5</sub> ResNet20	float	80.64%	58.14%	50.32%	66.96%
	BC	75.54%	51.03%	46.01%	60.92%
	BR	75.40%	51.60%	46.91%	61.52%

TABLE I: Binary Connect vs Binary Relax

paring to the ResNet with the samiliar number of parameters under quantization. We train two sets of  $\text{EnResNet}$  and ResNet with adversarial training. As shown in table II,  $\text{EnResNet}$  has much higher robust accuracy for both float and quantized models. We also study the behavior of quantized models under black-box attacks. Suppose we have a target model and a oracle model. We test a quantized target network by three different blind attacks. The oracle models are the float equivalent of the target model, a quantized model with different architecture (to the target model), and a float model with different architecture respectively. The results are in Table III. We observe that accuracies of models are improved significantly comparing those of white-box attack.

net(#params)	model	$N$	$A_1$	$A_2$	$A_3$
En <sub>1</sub> ResNet20(0.27M)	float	78.31%	56.61%	49.00%	66.84%
	br	69.60%	47.17%	43.89%	58.79%
ResNet20(0.27M)	float	76.30%	51.19%	46.72%	57.90%
	br	66.81%	43.37%	40.72%	52.14%
En <sub>2</sub> ResNet20(0.54M)	float	80.10%	57.48%	49.36%	66.73%
	br	72.58%	49.29%	44.72%	60.36%
ResNet34(0.56M)	float	77.82%	54.05%	49.89%	61.38%
	br	70.31%	46.42%	43.26%	54.75%

TABLE II: Ensemble ResNet vs ResNets

Target	Oracle	$A_1$	$A_2$	$A_3$
En <sub>2</sub> ResNet20	En <sub>2</sub> ResNet20 Float	59.88%	55.65%	66.06%
En <sub>2</sub> ResNet20	En <sub>3</sub> ResNet20 Binary	55.18%	52.74%	65.82%
En <sub>2</sub> ResNet20	En <sub>3</sub> ResNet20 Float	59.58%	55.59%	65.83%
En <sub>5</sub> ResNet20	En <sub>5</sub> ResNet20 Float	61.30%	57.05%	68.14%
En <sub>5</sub> ResNet20	En <sub>1</sub> ResNet20 Binary	58.96%	56.54%	68.14%
En <sub>5</sub> ResNet20	En <sub>1</sub> ResNet20 Float	61.58%	57.72%	69.82%

**TABLE III:** Robustness of binarized models under Black Box Attack

### C. Adaptation of Existing analysis of BC to adversarial training

Researchers have established quite a few theoretical on stability of training binary DNNs and error bounds of binary DNNs. We remark that these theoretical analysis of quantization under natural training can be adapted to adversarial training.

We use short-hand  $h(w, x_n)$  for  $\max_{\tilde{x}_n \in D_n} l(f(w, \tilde{x}_n), y_n)$ . Consequently, we rewrite (3) more concisely as:

$$\min_w \mathcal{L}(w) = \frac{1}{N} \sum_{n=1}^N h(w, x_n)$$

We first introduce a few common assumptions used in analysis of DNNs.

#### Assumptions:

- 1)  $h$  is Lipschitz differentiable in both arguments. i.e.  $\exists C > 0$  s.t.
 
$$\sup_x \|\nabla_w h(w_1, x) - \nabla_w h(w_2, x)\| \leq C \|w_1 - w_2\|$$

$$\sup_w \|\nabla_w h(w, x_1) - \nabla_w h(w, x_2)\| \leq C \|x_1 - x_2\|$$

$$\sup_x \|\nabla_x h(w_1, x) - \nabla_x h(w_2, x)\| \leq C \|w_1 - w_2\|$$
- 2) The variance of the stochastic gradients is bounded. i.e.  $\mathbb{E}[\|\nabla \mathcal{L}(w) - \nabla \mathcal{L}_k(w)\|^2] \leq \sigma^2, \forall k \in \mathbb{N}$ , where  $\nabla \mathcal{L}_k(w)$  is the sampled mini-batch gradient at  $k$ -th epoch.
- 3)  $h(w, x)$  is locally strongly concave in  $x$  in all  $D_n$ . That is,  $\exists \mu > 0$  s.t.  $\forall n$  and  $x_1, x_2 \in D_n$ , we have
 
$$h(w, x_1) \geq h(w, x_2) + \langle \nabla_x h(w, x_2), x_1 - x_2 \rangle - \frac{\mu}{2} \|x_1 - x_2\|^2$$

Lipschitz differentiable and bounded variance of stochastic gradients are common assumptions [27], [14], [25], [20] made for analysis of gradient descent. Assumption 3, made according to [20], [25], is the additional assumption to adapt the situation to robust training.

**Lemma 1** (lemma 1 in [25]). *Under assumption 1 and 3, we have  $\mathcal{L}$  is  $L$ -Lipschitz differentiable*

$$\|\nabla \mathcal{L}(w_1) - \nabla \mathcal{L}(w_2)\| \leq L \|w_1 - w_2\|$$

then consequently,

$$\mathcal{L}(w_1) \leq \mathcal{L}(w_2) + \langle \nabla \mathcal{L}(w_2), w_1 - w_2 \rangle + \frac{L}{2} \|w_1 - w_2\|^2$$

where  $L = \frac{C^2}{\mu} + C$

Lemma 1 shows that if the original loss function is Lipschitz differentiable, with a few additional conditions, the loss function of adversarial training is also Lipschitz differentiable. This result allows us to extend many existing analysis of

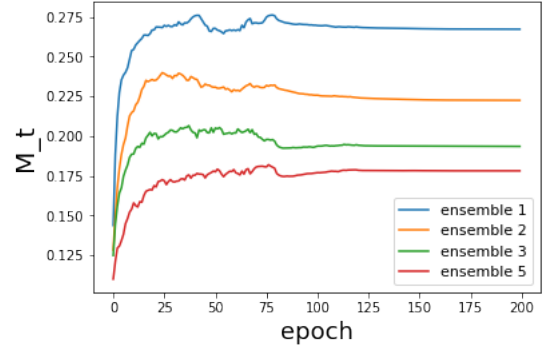


**Fig. 2:** Maximum of Binary Weights under  $l_1$  norm against epochs

quantization to adversarial training. In particular, the following theorem provided by [14] holds for adversarial training.

**Theorem 1** (Theorem 3 in [14]). *Let  $w^* = \operatorname{argmin}_{w \in R^n} \mathcal{L}(w)$  and learning rate  $\gamma_t = \frac{1}{t}$ . Assume that the domain of  $\mathcal{L}$  is bounded with diameter  $D$ .  $\mathcal{L}$  is convex and satisfies the assumptions 1,2 and 3, then the ergodic error satisfies*

$$\lim_{T \rightarrow \infty} \mathbb{E}[\mathcal{L}(\bar{w}_T) - \mathcal{L}(w^*)] \leq 2\sqrt{n}MLD$$

where  $\bar{w}_T = \frac{1}{T} \sum_{t=1}^T w_t$ ,  $L$  and  $M$  are the constants in Lemma 1 and  $\limsup_t \mathbb{E}[\|w_t\|]$  respectively, and  $n$  is the dimension of the domain.

Network	M
En <sub>1</sub> ResNet20	0.2762
En <sub>2</sub> ResNet20	0.2399
En <sub>3</sub> ResNet20	0.2065
En <sub>5</sub> ResNet20	0.1819

**TABLE IV:** the uniform bound  $M$

One drawback of this theorem is that whether  $M$  is bounded or not remains unknown to us. Therefore, we numerically investigate the values of  $M$ , and we uncover an interesting feature of ensemble ResNet. Let  $\mathcal{W}_t$  be collection of convolutional layers of the neural network at epoch  $t$ . Define

$$M_t = \max_{w \in \mathcal{W}_t} E(|w|), \quad M = \max_{1 \leq t \leq T} \mathbb{E}(|w|) = \max_{1 \leq t \leq T} M_t$$

Since we train each model 200 epochs, we have  $T = 200$  here. We find that  $M$  is numerically bounded (as in Fig. 2) and small. Moreover, the value of  $M$  decreases as the number of ensembles increases (Table IV). In other words, the bound provided by theorem 1 is tighter when the number of ensembles is larger. From Table 3, we see that, for both quantized and float model the kernels have the smaller weights for the larger number of ensembles. A pervious work that studied the sparsity of EnResNet [6] also found a similar result that the weights of EnResNet are smaller for a larger number of ensembles. Theorem 1 offers an explanation that how this feature of EnResNet can favor its performance.

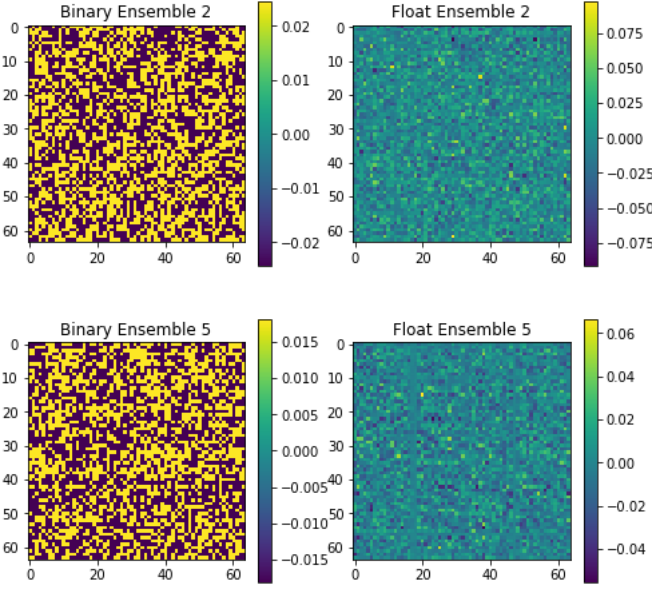


**Fig. 3:** Visualizations of float and quantized kernels: left-hand side columns are randomly selected kernels of quantized models, and the right-hand columns are the same kernels of float models

#### IV. TRADE-OFF BETWEEN ROBUST ACCURACY AND NATURAL ACCURACY

##### A. Previous work and our methodology

It is known that adversarial training will decrease the accuracy for clean input data. This phenomenon is verified both theoretically [22] and experimentally [28], [24], [13] by researchers. [28] proposed a trade of loss function for robust training to balance the adversarial accuracy and natural accuracy. It formulated as following:

$$\mathcal{L} = \mathcal{L}_{nat} + \beta \cdot \frac{1}{N} \sum_{n=1}^N l(f(x_n), f(\tilde{x}_n)) \quad (5)$$

Motivated by [28], we study the following trade-off loss function for our quantized models:

$$\mathcal{L} = \alpha \cdot \mathcal{L}_{nat} + \beta \cdot L_{rob} \quad (6)$$

Note that adversarial training is a special case  $\alpha = 0, \beta = 1$  in (6).

##### B. Experiment and result

To compare the performances of two loss functions, we fix our network and dataset to be  $\text{En}_1\text{ResNet20}$  and CIFAR-10. Based on [28], who studied  $\beta$  of (5) in the range  $[1, 10]$ , we set the trade-off parameter  $\beta \in [1, 4, 8]$  to emphasize the robustness in different levels.

The experiment results are in Table V. We observe that, when the natural loss and the adversarial loss are equally treated, (5) focuses on the natural accuracy while (6) favors on the robust accuracy. As the trade-off parameter  $\beta$  increases, (5) trades quite amount of natural loss for robustness, while (6) trades a relatively small amount of natural loss for robustness. In another word, we find that (6) has better trade-off efficiency. Hence, we say that the loss function (6) outperforms (5).

##### C. Analysis of trade-off functions

Let us consider the binary classification case, where have our samples  $(\mathbf{x}, y) \in \mathcal{X} \times \{-1, 1\}$ . Let  $f: \mathcal{X} \rightarrow \mathbb{R}$  be a classifier and  $\sigma(\cdot)$  be an activation function. Then our prediction for a sample is  $\hat{y} = \text{sign}(f(\mathbf{x}))$  and the corresponding score is  $\sigma(f(\mathbf{x}))$ . Above is the theoretical setting provided by [28]. Then, we have the errors  $\mathcal{R}_\phi(f)$  and  $\mathcal{R}_\phi^*(f)$  corresponding to (5) and (6) respectively, considering  $\alpha = \beta = 1$  for both loss functions:

$$\mathcal{R}_\phi(f) = \mathbb{E}[\phi(\sigma \circ f(\mathbf{x}) \cdot y)] + \mathbb{E}[\phi(\sigma \circ f(\mathbf{x}) \cdot \sigma \circ f(\mathbf{x}'))]$$

$$\mathcal{R}_\phi^*(f) = \mathbb{E}[\phi(\sigma \circ f(\mathbf{x}) \cdot y)] + \mathbb{E}[\phi(\sigma \circ f(\mathbf{x}') \cdot y)]$$

We first consider the simple case that  $\phi$  is the 0-1 loss function. Then, we don't need a activation function in this case so we take  $\sigma(\theta) = \theta$ .

**Proposition 1.** *Let  $\phi$  be the 0-1 loss function and activation function be the identity map. Then,*

$$\mathcal{R}_\phi(f) \leq \mathcal{R}_\phi^*(f)$$

*Proof:* We first define a set  $E$ :

$$E = \{\mathbf{x} | f(\mathbf{x})y < 0, f(\mathbf{x}')y > 0\}$$

By the definition of adversarial examples in (3),

$$\mathbb{E}[\mathbf{1}\{E\}] = 0$$

where  $\mathbf{1}\{E\}$  is the indicator function of the set. That is, the set that the classifier predicts original data point wrong but the perturbed data point correctly should have measure 0. Now, we define the following sets:

$$B = \{\mathbf{x} | f(\mathbf{x})y \geq 0, f(\mathbf{x}')y \geq 0\}$$

$$D = \{\mathbf{x} | f(\mathbf{x})y \geq 0, f(\mathbf{x}')y < 0\}$$

$$F = \{\mathbf{x} | f(\mathbf{x})y < 0, f(\mathbf{x}')y < 0\}$$

We note that

$$\{\exists \mathbf{x}' \in \mathbf{B}(\mathbf{x}, \delta) \ f(\mathbf{x}')f(\mathbf{x}) \leq 0\} = D \cup E$$

$$\{\exists \mathbf{x}' \in \mathbf{B}(\mathbf{x}, \delta) \ f(\mathbf{x}')y \leq 0\} = D \cup F$$

Then

$$\mathbb{E}[\mathbf{1}\{\exists \mathbf{x}' \in \mathbf{B}(\mathbf{x}, \delta) \ f(\mathbf{x}')f(\mathbf{x}) \leq 0\}] = \mathbb{E}[\mathbf{1}\{D\}]$$

$$\leq \mathbb{E}[\mathbf{1}\{D\} + \mathbf{1}\{F\}] = \mathbb{E}[\mathbf{1}\{\exists \mathbf{x}' \in \mathbf{B}(\mathbf{x}, \delta) \ f(\mathbf{x}')y \leq 0\}]$$

As we consider the naive 0-1 loss, both loss functions have no penalty on set  $B$ . Therefore, we have

$$\mathcal{R}_\phi(f) = \mathbb{E}[\mathbf{1}\{f(\mathbf{x})y \leq 0\} + \mathbf{1}\{\exists \mathbf{x}' \in \mathbf{B}(\mathbf{x}, \delta) \ f(\mathbf{x}')f(\mathbf{x}) \leq 0\}]$$

$$\leq \mathbb{E}[\mathbf{1}\{f(\mathbf{x})y \leq 0\} + \mathbf{1}\{\exists \mathbf{x}' \in \mathbf{B}(\mathbf{x}, \delta) \ f(\mathbf{x}')y \leq 0\}] = \mathcal{R}_\phi^*(f)$$

□

The underlying message behind these results is that under the same classifier, loss function and activation function,  $\mathcal{R}_\phi^*(f)$  captures more errors than  $\mathcal{R}_\phi(f)$ , as the later fails to capture the robust error when the natural prediction is incorrect.

Net	Loss	$N$	$A_1$	$A_2$	$A_3$
En <sub>1</sub> ResNet20	(5) ( $\beta = 1$ )	<b>84.49%</b>	45.96%	34.81%	51.94%
En <sub>1</sub> ResNet20	(6) ( $\alpha = 1, \beta = 1$ )	83.47%	<b>54.46%</b>	<b>43.86%</b>	<b>64.04%</b>
En <sub>1</sub> ResNet20	(5) ( $\beta = 4$ )	80.05%	51.24%	45.43%	58.85%
En <sub>1</sub> ResNet20	(6) ( $\alpha = 1, \beta = 4$ )	<b>80.91%</b>	<b>55.92%</b>	<b>47.77%</b>	<b>66.53%</b>
En <sub>1</sub> ResNet20	(5) ( $\beta = 8$ )	75.82%	51.63%	46.95%	59.31%
En <sub>1</sub> ResNet20	(6) ( $\alpha = 1, \beta = 8$ )	<b>79.31%</b>	<b>56.28%</b>	<b>47.82%</b>	<b>66.07%</b>

TABLE V: Comparison of Loss Function

The same result also holds in more general cases. Now, we consider several common loss functions: the hinge loss ( $\phi(\theta) = \max\{1 - \theta, 0\}$ ), the sigmoid loss ( $\phi(\theta) = 1 - \tanh \theta$ ), and the logistic loss ( $\phi(\theta) = \log_2(1 + e^{-\theta})$ ). Note that we want a loss function to be monotonic decreasing in  $[-1, 1]$  as  $-1$  indicates completely wrong and  $1$  indicates completely correct. Since our classes is  $1$  and  $-1$ , we will choose hyperbolic tangent as our activation function.

**Proposition 2.** *Let  $\phi$  be any loss function that is monotonic decreasing on  $[-1, 1]$  (all loss functions mentioned above satisfy this), and  $\sigma(\theta) = \tanh \theta$ . Define  $B = \{\mathbf{x} | f(\mathbf{x})y \geq 0, f(\mathbf{x}')y \geq 0\}$  as in proposition 1. Then:*

$$\mathcal{R}_\phi(f) \geq \mathcal{R}_\phi^*(f) \text{ on } B \text{ and } \mathcal{R}_\phi(f) \leq \mathcal{R}_\phi^*(f) \text{ on } B^C$$

*Proof:* Let  $E$ ,  $D$ , and  $F$  be the sets defined in proposition 1. We note that the activation function  $\sigma(x)$  preserves the sign of  $x$ , and  $|\sigma(x)| \leq 1$ .

On the set  $B$ ,  $f(\mathbf{x})$ ,  $f(\mathbf{x}')$ , and  $y$  have the same sign, so are  $\sigma(f(\mathbf{x}))$ ,  $\sigma(f(\mathbf{x}'))$  and  $y$ . Therefore

$$\phi(\sigma(f(\mathbf{x}')) \cdot \sigma(f(\mathbf{x}))) \geq \phi(\sigma(f(\mathbf{x}') \cdot y))$$

as  $0 \leq \sigma(f(\mathbf{x}')) \cdot \sigma(f(\mathbf{x})) \leq \sigma(f(\mathbf{x}') \cdot y)$ . This shows

$$\mathcal{R}_\phi(f) \geq \mathcal{R}_\phi^*(f) \text{ on } B$$

We note that  $B^C = E \cup D \cup F$ . Since set  $E$  has measure zero, we only consider  $D$  and  $F$ .

On  $D$ , as  $f$  classifies  $\mathbf{x}$  correct and  $\mathbf{x}'$  wrong, we have

$$\begin{aligned} \sigma(f(\mathbf{x}')) \cdot y &\leq \sigma(f(\mathbf{x}')) \cdot \sigma(f(\mathbf{x})) \leq 0 \\ \Rightarrow \phi(\sigma(f(\mathbf{x}')) \cdot \sigma(f(\mathbf{x}))) &\leq \phi(\sigma(f(\mathbf{x}') \cdot y)) \end{aligned}$$

On  $F$ , as  $f$  classifies both  $\mathbf{x}$  and  $\mathbf{x}'$  wrong, we have

$$\begin{aligned} \sigma(f(\mathbf{x}')) \cdot y &\leq 0 \leq \sigma(f(\mathbf{x}')) \cdot \sigma(f(\mathbf{x})) \\ \Rightarrow \phi(\sigma(f(\mathbf{x}')) \cdot \sigma(f(\mathbf{x}))) &\leq \phi(\sigma(f(\mathbf{x}') \cdot y)) \end{aligned}$$

In summary, we have

$$\mathcal{R}_\phi(f) \leq \mathcal{R}_\phi^*(f) \text{ on } B^C$$

□

In the more general case of proposition 2, we partition our space into several sets based on a given classifier  $f$ , and we examine the actions of loss functions on those sets. We see that (5) penalize set  $B$  heavier than (6), but the classifier classifies both the natural data and the perturbed data correct on  $B$ . On the other hand, (5) does not penalize sets  $E$  and  $F$ , where the classifier makes mistakes, enough, especially on set  $F$ .

Therefore, (6) as a loss function is more on target. Based on both experimental results and theoretical analysis, we believe (6) is a better choice to balance natural accuracy and robust accuracy.

As our experiment on the balance of accuracies with different parameters in our loss function (6) in table VI. We find that it is possible to increase the natural accuracy while maintaining the robustness under relatively weak attacks (FGSM & CW), as the case of  $\alpha = 1$  and  $\beta = 8$  in table VI. However, the resistance under relatively strong attack (IFGSM) will inevitably decrease when we trade-off.

net	loss	$N$	$A_1$	$A_2$	$A_3$
En <sub>1</sub> ResNet20	$\alpha = 0, \beta = 1$	69.60%	<b>47.81%</b>	<b>43.89%</b>	58.79%
En <sub>1</sub> ResNet20	$\alpha = 1, \beta = 4$	<b>73.40%</b>	47.41%	41.86%	57.83%
En <sub>1</sub> ResNet20	$\alpha = 1, \beta = 8$	71.35%	47.42%	42.46%	<b>59.01%</b>
En <sub>2</sub> ResNet20	$\alpha = 0, \beta = 1$	71.58%	49.29%	<b>44.62%</b>	60.36%
En <sub>2</sub> ResNet20	$\alpha = 1, \beta = 4$	<b>75.92%</b>	48.97%	43.41%	59.40%
En <sub>2</sub> ResNet20	$\alpha = 1, \beta = 8$	74.72%	<b>49.66%</b>	43.96%	<b>60.65%</b>
En <sub>5</sub> ResNet20	$\alpha = 0, \beta = 1$	75.40%	51.60%	<b>46.91%</b>	<b>61.52%</b>
En <sub>5</sub> ResNet20	$\alpha = 1, \beta = 4$	<b>78.50%</b>	50.85%	45.02%	60.96%
En <sub>5</sub> ResNet20	$\alpha = 1, \beta = 8$	77.35%	<b>51.62%</b>	45.63%	61.11%

TABLE VI: Trade-off loss function for quantized models

## V. FURTHER BALANCE OF EFFICIENCY AND ROBUSTNESS: STRUCTURED SPARSE QUANTIZED NEURAL NETWORK VIA TERNARY/4-BIT QUANTIZATION AND TRADE-OFF LOSS FUNCTION

### A. Sparse neural network delivered by high precision quantization

If we quantize DNNs with higher precision than binary quantization, such as ternary and 4-bit quantization. Then, the quantized weights are allowed to be 0. In fact, we find that a large proportion of weights will be 0 for quantized models. This suggests that a ternary or 4-bit quantized model can be further simplified via channel pruning. However, such simplification requires structure sparsity of DNN architecture. In our study, we use the algorithm 1 as before with the projection replaced by ternary and 4-bit respectively. As shown in Table VII, we find that sparsity of quantized DNNs under regular training are significantly more structured than those under adversarial training. For both ternary(tnn) and 4-bit quantization, quantized models with adversarial training have very unstructured sparsity, while models with natural training have much more structured sparsity. We verify this phenomenon for both ResNet20, En<sub>1</sub>ResNet20, ResNet56, and En<sub>1</sub>ResNet56. For example, 50.71% (0.135M out of 0.268M) of weights in convolutional layers are 0 in a ternary quantized ResNet20, but there are only 2.55% (16 out of 627) channels are 0. If the sparsity is unstructured, it is useless for model



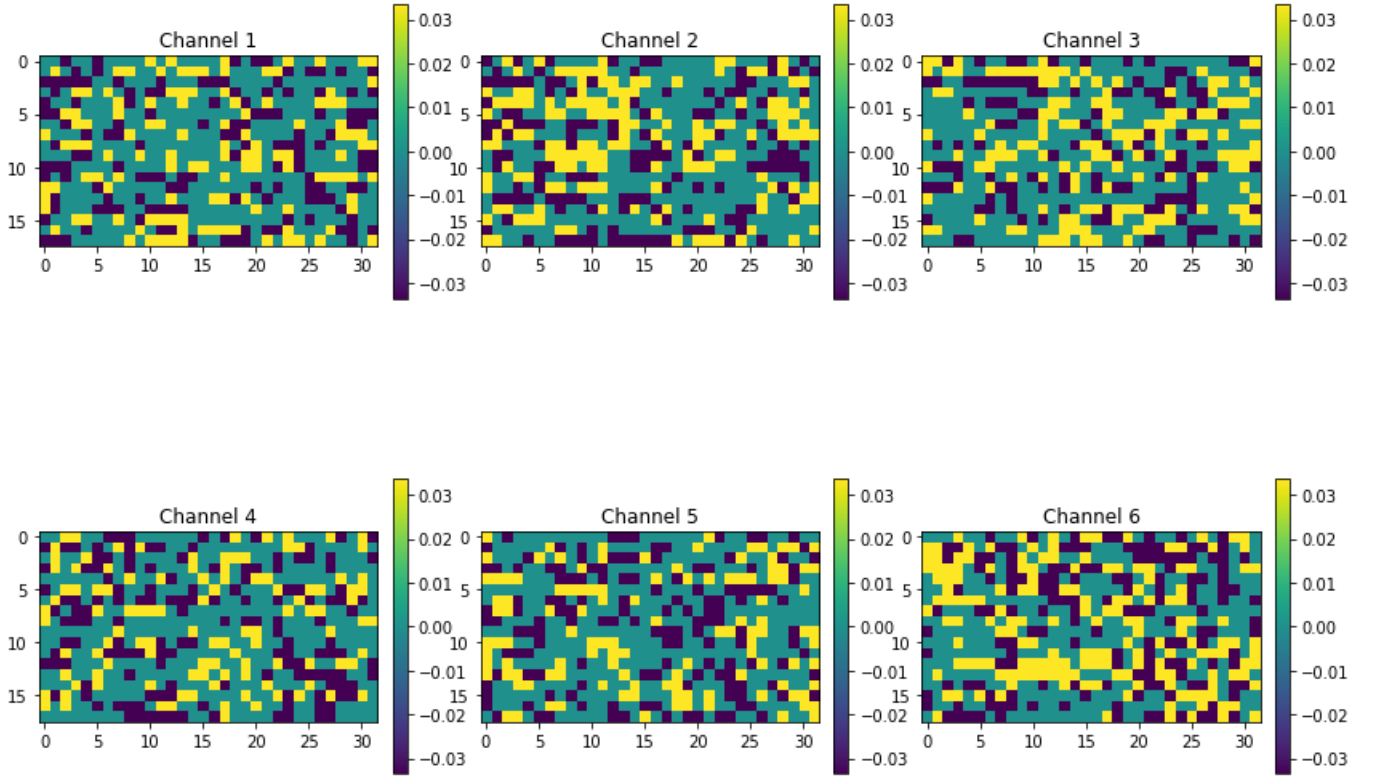


**Fig. 4:** Visualization of 4 ternary channels (reshaped for visualization) of a layer in ResNet20 under AT. The green areas are 0 weights.

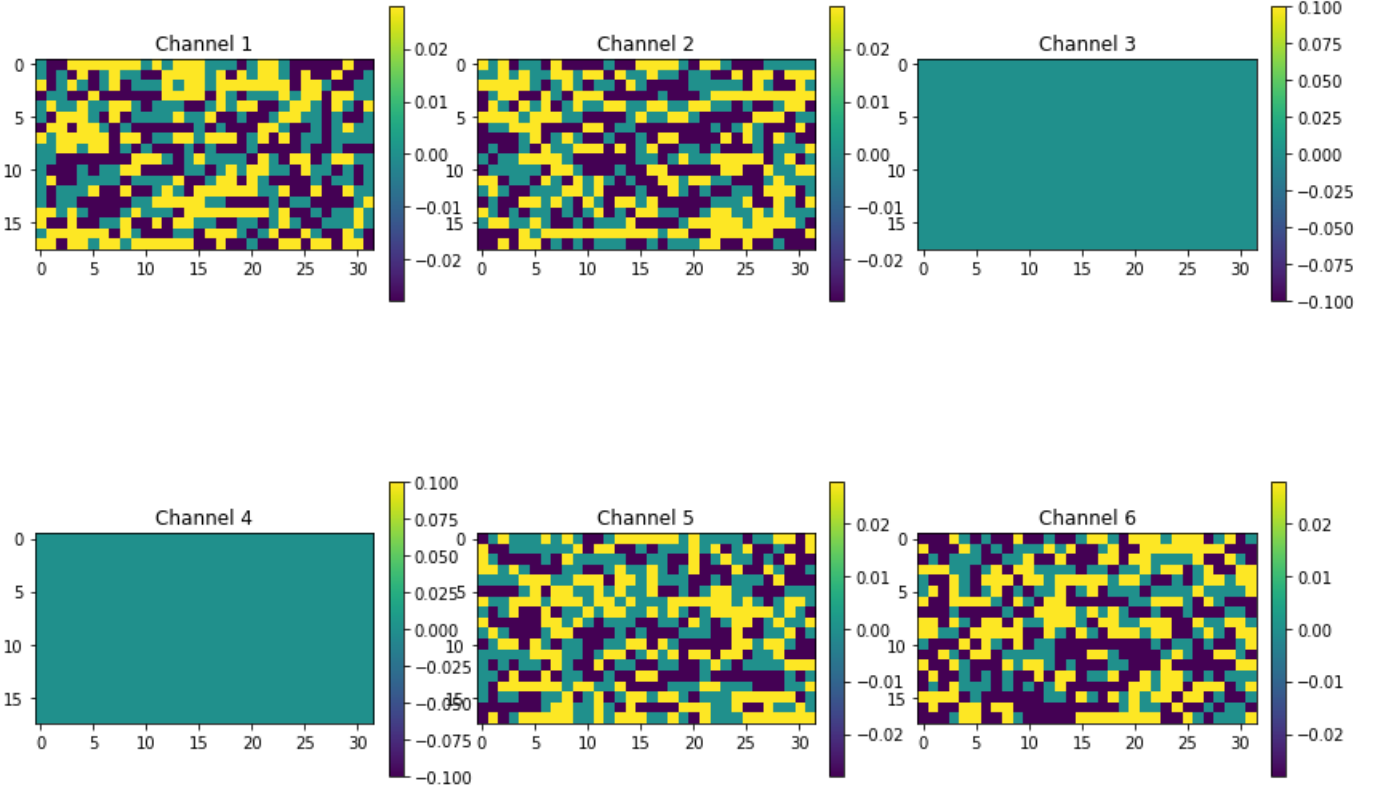


**Fig. 5:** Visualization of 4 ternary channels (reshaped for visualization) of a layer in  $\text{En}_1\text{ResNet56}$  under natural training. There are less 0 weights in non-sparse channels.

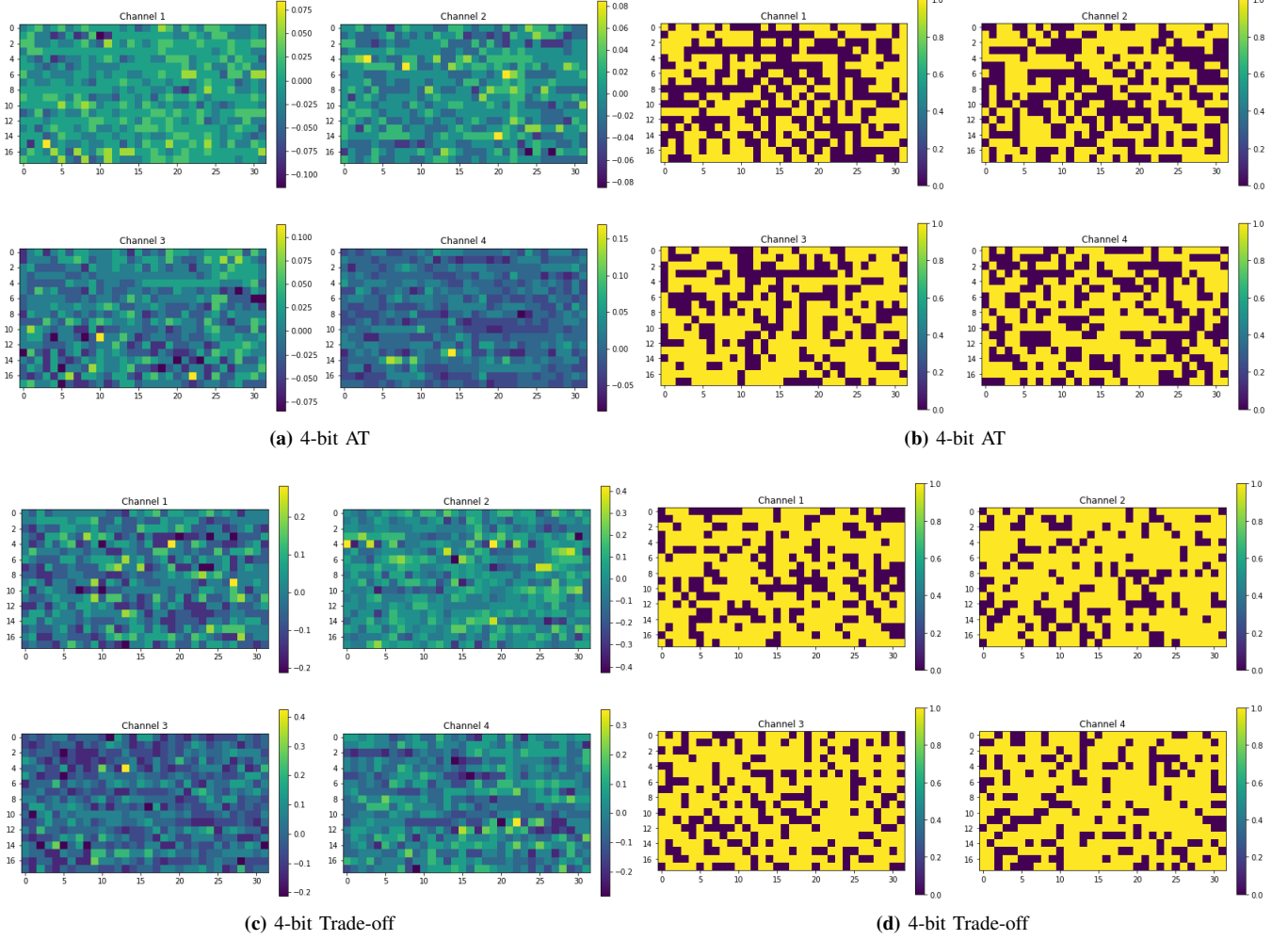


**Fig. 6:** Comparison of Adversarial training (AT) with trade-off loss: the left-hand side are original plots of channels, and we isolate the zero weights and nonzero weights of the left-hand side channels for better visualization in right-hand side. The dark parts are zero weights and the yellow parts are nonzero weights

simplification as channel pruning cannot be applied. A fix to this problem is our trade-off loss function, as factor natural loss into adversarial training should improve the structure of sparsity. Our experiment (Table VII) shows that a small factor of natural loss,  $\alpha = 1$  and  $\beta$  in (6), can push the sparsity to be more structured. Meanwhile, the deepness of models also has an impact on the structure of sparsity. The deeper the more structured the sparsity is. We see in Table VII that, under the same setting, the structure of sparsity increases as the model becomes deeper. Also,  $\text{En}_5\text{ResNet20}$  and  $\text{En}_2\text{ResNet56}$  (with trade-off loss) in Table VIII have much more channel sparsity than  $\text{En}_1\text{ResNet20}$  and  $\text{En}_1\text{ResNet56}$  (with trade-off loss) respectively. Figure 4 and figure 5, shows the difference between a unstructured sparsity of a ternary ResNet20 with adversarial training and a much more structured sparsity of ResNet56 with natural training.

### B. Further study and generalization

Based on previous discussions, together with quantization and our trade-off loss function, we can produce very efficient

DNN models with high robustness. The trade-off function not only improves the natural accuracy of models with minor harm to robustness but also structure the sparsity of high precision quantization, so further simplification of models can be done through channel pruning. Now, we want to generalize our result to more datasets. We verify that the performance of the quantized model with our trade-off loss function can be generalize to other popular datasets, including Cifar 100 [11], MNIST, Fashion MNIST (FMNIST) [26], and SVHN [18]. Among these datasets, MNIST and Fashion-MNIST are digital images with only one channel, i.e. black-and-white, and, therefore, are much easier to learn than CIFAR10. The Street View House Numbers(SVHN) datasets are images with three RGB channels, color digital images, like CIFAR10. In our experiments, we learn SVHN dataset without utilizing its extra training data. As Fashion-MNIST and SVHN are somewhat less popular than MNIST and CIRFAR10, we visualize each dataset with a mini-batch in Figure(7). Last, we test our quantized model on a large dataset CIFAR100, which contains 100 classes with 600 images per class. Our

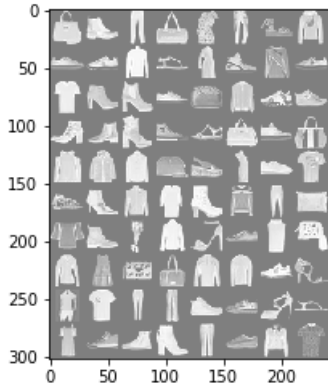


Net	Quant	Loss	Weight Sparsity	Channel Sparsity	$N$	$A_1$	$A_2$
ResNet20	tnn	Natural	53.00%	11.16%	90.54%	12.71%	0.00%
En <sub>1</sub> ResNet20	tnn	Natural	52.19%	9.57%	90.61%	26.21%	0.71%
ResNet20	tnn	AT	50.71%	2.55%	68.30%	44.80%	42.53%
En <sub>1</sub> ResNet20	tnn	AT	50.31%	4.14%	71.30%	48.17%	43.27%
En <sub>1</sub> ResNet20	tnn	(6)	55.66%	7.02%	73.05%	48.10%	42.65%
ResNet20	4-bit	Natural	42.79%	9.53%	91.75%	12.38%	0.00%
En <sub>1</sub> ResNet20	4-bit	Natural	44.73%	10.52%	91.42%	27.99%	0.62%
ResNet20	4-bit	AT	43.93%	2.55%	71.49%	47.63%	44.08%
En <sub>1</sub> ResNet20	4-bit	AT	48.35%	4.94%	73.05%	51.43%	45.10%
En <sub>1</sub> ResNet20	4-bit	(6)	55.57%	7.42%	76.61%	51.92%	44.39%
ResNet56	tnn	Natural	60.96%	31.86%	91.91%	15.58%	0.00%
En <sub>1</sub> ResNet56	tnn	Natural	60.66%	28.97%	91.46%	38.22%	0.36%
ResNet56	tnn	AT	54.21%	15.37%	74.56%	51.73%	46.62%
En <sub>1</sub> ResNet56	tnn	AT	54.70%	16.74%	76.87%	53.16%	47.89%
En <sub>1</sub> ResNet56	tnn	(6)	58.89%	21.36%	77.24%	52.96%	46.01%
ResNet56	4-bit	Natural	67.94%	39.16%	93.09%	16.02%	0.00%
En <sub>1</sub> ResNet56	4-bit	Natural	71.07%	41.10%	92.39%	39.79%	0.33%
ResNet56	4-bit	AT	55.29%	17.10%	77.67%	52.43%	48.22%
En <sub>1</sub> ResNet56	4-bit	AT	55.09%	18.11%	78.25%	55.48%	49.03%
En <sub>1</sub> ResNet56	4-bit	(6)	67.31%	33.18%	79.44%	55.41%	47.80%

TABLE VII: Sparsity and structure of sparsity of quantized models. We use  $\alpha = 1$  and  $\beta = 8$  in trade-off loss (6)



(a) SVHN



(b) Fashion-MNIST

Fig. 7: a mini-batch of SVHN dataset and a mini-batch of Fashion-MNIST dataset

results are displayed in Table VIII. We find that binary models are almost as good as the float models on the small datasets MNIST and Fashion MNIST. Unfortunately, binary models do not do well in large difficult datasets like SVNH and Cifar100,

but 4-bit quantized models have comparable performances as float ones. Although 4-bit quantization requires higher precision, the highly structured sparsity can quite compensate the efficiency of models.

## VI. CONCLUSION

In this paper, we study the robustness of quantized models. The experimental results suggest that quantized models are not more vulnerable under adversarial attacks, and a well-designed trade-off function can increase the natural accuracy of a model with minor reduction of robustness. Moreover, we discover that high precision quantization can offer sparse DNNs, and a trade-off function can make this sparsity structured. By combining a powerful robust model, EnResNet, and our trade-off loss function, we find that keeping a model both efficient and robust is promising and worth paying attention to. We hope our study can serve as a benchmark for future studies on this interesting topic.

## REFERENCES

- [1] Anish Athalye, Nicholas Carlini, and David Wagner. Obfuscated gradients give a false sense of security: Circumventing defenses to adversarial examples. *arXiv preprint arXiv:1802.00420*, 2018.
- [2] Anish Athalye, Logan Engstrom, Andrew Ilyas, and Kevin Kwok. Synthesizing robust adversarial examples. *arXiv preprint arXiv:1707.07397*, 2017.
- [3] Nicholas Carlini and David Wagner. Towards evaluating the robustness of neural networks. In *2017 IEEE Symposium on Security and Privacy (SP)*, pages 39–57. IEEE, 2017.
- [4] T. Chen, Y. Rubanova, J. Bettencourt, and D. Duvenaud. Neural ordinary differential equations. In *Advances in neural information processing systems*, pages 6571–6583, 2018.
- [5] Matthieu Courbariaux, Yoshua Bengio, and Jean-Pierre David. Binaryconnect: Training deep neural networks with binary weights during propagations. In *Advances in neural information processing systems*, pages 3123–3131, 2015.
- [6] Thu Dinh, Bao Wang, Andrea L Bertozzi, Stanley J Osher, and Jack Xin. Sparsity meets robustness: Channel pruning for the feynman-kac formalism principled robust deep neural nets. *arXiv preprint arXiv:2003.00631*, 2020.
- [7] Ian J Goodfellow, Jonathon Shlens, and Christian Szegedy. Explaining and harnessing adversarial examples. *arXiv preprint arXiv:1412.6572*, 2014.

net	dataset	Quantization	Channel Sparsity	N	$A_1$	$A_2$	$A_3$
En <sub>2</sub> ResNet20	MNIST	BR	N/A	99.22%	98.90%	98.90%	99.12%
En <sub>2</sub> ResNet20	MNIST	Float	N/A	99.21%	99.02%	98.91%	99.14%
En <sub>2</sub> ResNet20	FMNIST	BR	N/A	91.69%	87.85%	87.22%	90.44%
En <sub>2</sub> ResNet20	FMNIST	Float	N/A	92.74%	89.35%	88.68%	91.72%
En <sub>5</sub> ResNet20	Cifar10	4-bit	35.24%	76.77%	54.03%	48.12%	63.74%
En <sub>5</sub> ResNet20	Cifar10	tnn	18.18%	76.65%	52.99%	46.88%	62.69%
En <sub>5</sub> ResNet20	Cifar10	Float	N/A	80.64%	58.14%	50.32%	66.96%
En <sub>2</sub> ResNet56	Cifar100	4-bit	43.94%	52.24%	29.29%	24.46%	39.49%
En <sub>2</sub> ResNet56	Cifar100	Float	N/A	55.65%	31.83%	27.07%	40.79%
En <sub>2</sub> ResNet56	SVHN	4-bit	49.03%	91.21%	70.91%	57.99%	72.44%
En <sub>2</sub> ResNet56	SVHN	Float	N/A	93.33%	78.08%	58.11%	75.79%

**TABLE VIII:** Generalization of quantized models to more datasets. All models are trained with loss (6)  $\alpha = 1$  and  $\beta = 8$

- [8] Chuan Guo, Mayank Rana, Moustapha Cisse, and Laurens Van Der Maaten. Countering adversarial images using input transformations. *arXiv preprint arXiv:1711.00117*, 2017.
- [9] Kaiming He, Xiangyu Zhang, Shaoqing Ren, and Jian Sun. Deep residual learning for image recognition. In *Proceedings of the IEEE conference on computer vision and pattern recognition*, pages 770–778, 2016.
- [10] Yihui He, Xiangyu Zhang, and Jian Sun. Channel pruning for accelerating very deep neural networks. In *Proceedings of the IEEE International Conference on Computer Vision*, pages 1389–1397, 2017.
- [11] Alex Krizhevsky et al. Learning multiple layers of features from tiny images. 2009.
- [12] Alexey Kurakin, Ian Goodfellow, and Samy Bengio. Adversarial examples in the physical world. *arXiv preprint arXiv:1607.02533*, 2016.
- [13] Alexey Kurakin, Ian Goodfellow, and Samy Bengio. Adversarial machine learning at scale. *arXiv preprint arXiv:1611.01236*, 2016.
- [14] Hao Li, Soham De, Zheng Xu, Christoph Studer, Hanan Samet, and Tom Goldstein. Training quantized nets: A deeper understanding. In *Advances in Neural Information Processing Systems*, pages 5811–5821, 2017.
- [15] Yandong Li, Lijun Li, Liqiang Wang, Tong Zhang, and Boqing Gong. Nattack: Learning the distributions of adversarial examples for an improved black-box attack on deep neural networks. *arXiv preprint arXiv:1905.00441*, 2019.
- [16] Z. Li and Z. Shi. Deep residual learning and pdes on manifold. *arXiv preprint arXiv:1708.05115*, 2017.
- [17] Aleksander Madry, Aleksandar Makelov, Ludwig Schmidt, Dimitris Tsipras, and Adrian Vladu. Towards deep learning models resistant to adversarial attacks. *arXiv preprint arXiv:1706.06083*, 2017.
- [18] Yuval Netzer, Tao Wang, Adam Coates, Alessandro Bissacco, Bo Wu, and Andrew Y Ng. Reading digits in natural images with unsupervised feature learning. 2011.
- [19] Mohammad Rastegari, Vicente Ordonez, Joseph Redmon, and Ali Farhadi. Xnor-net: Imagenet classification using binary convolutional neural networks. In *European conference on computer vision*, pages 525–542. Springer, 2016.
- [20] Aman Sinha, Hongseok Namkoong, and John Duchi. Certifying some distributional robustness with principled adversarial training. *arXiv preprint arXiv:1710.10571*, 2017.
- [21] Christian Szegedy, Wojciech Zaremba, Ilya Sutskever, Joan Bruna, Dumitru Erhan, Ian Goodfellow, and Rob Fergus. Intriguing properties of neural networks. *arXiv preprint arXiv:1312.6199*, 2013.
- [22] Dimitris Tsipras, Shibani Santurkar, Logan Engstrom, Alexander Turner, and Aleksander Madry. Robustness may be at odds with accuracy. *arXiv preprint arXiv:1805.12152*, 2018.
- [23] B. Wang, X. Luo, Z. Li, W. Zhu, Z. Shi, and S. Osher. Deep neural nets with interpolating function as output activation. In *Advances in Neural Information Processing Systems*, pages 743–753, 2018.
- [24] Bao Wang, Zuoqiang Shi, and Stanley Osher. Resnets ensemble via the feynman-kac formalism to improve natural and robust accuracies. In *Advances in Neural Information Processing Systems*, pages 1655–1665, 2019.
- [25] Yisen Wang, Xingjun Ma, James Bailey, Jinfeng Yi, Bowen Zhou, and Quanquan Gu. On the convergence and robustness of adversarial training. In *International Conference on Machine Learning*, pages 6586–6595, 2019.
- [26] Han Xiao, Kashif Rasul, and Roland Vollgraf. Fashion-mnist: a novel image dataset for benchmarking machine learning algorithms. *arXiv preprint arXiv:1708.07747*, 2017.
- [27] Penghang Yin, Shuai Zhang, Jiancheng Lyu, Stanley Osher, Yingyong Qi, and Jack Xin. Binaryrelax: A relaxation approach for training deep neural networks with quantized weights. *SIAM Journal on Imaging Sciences*, 11(4):2205–2223, 2018.
- [28] Hongyang Zhang, Yaodong Yu, Jiantao Jiao, Eric P Xing, Laurent El Ghaoui, and Michael I Jordan. Theoretically principled trade-off between robustness and accuracy. *International Conference on Machine Learning*, 2019.
- [29] Zhuangwei Zhuang, Minghui Tan, Bohan Zhuang, Jing Liu, Yong Guo, Qingyao Wu, Junzhou Huang, and Jinhui Zhu. Discrimination-aware channel pruning for deep neural networks. In *Advances in Neural Information Processing Systems*, pages 875–886, 2018.